HHS Public Access

Author manuscript

Am J Ophthalmol. Author manuscript; available in PMC 2024 October 01.

Published in final edited form as:

Am J Ophthalmol. 2023 October ; 254: 11–22. doi:10.1016/j.ajo.2023.03.012.

Onset and Progression of Persistent Choroidal Hypertransmission Defects in Intermediate AMD: A Novel Clinical Trial Endpoint

Jeremy Liu[1], **Mengxi Shen**[1], **Rita Laiginhas**[1], **Gissel Herrera**[1], **Jianqing Li**[1], **Yingying Shi**[1], **Farhan Hiya**[1], **Omer Trivizki**[1], **Nadia K. Waheed**[2], **Carol Y. Chung**[3], **Eric M. Moult**[4], **James G. Fujimoto**[4], **Giovanni Gregori**[1], **Philip J. Rosenfeld**[1]

[1]Department of Ophthalmology, Bascom Palmer Eye Institute, University of Miami Miller School of Medicine, Miami, Florida, USA

[2]New England Eye Center, Tufts Medical Center, Tufts University School of Medicine, Boston, Massachusetts, USA

[3]Carol Chung Statistics Consulting, Inc., Pacifica, CA, USA

[4]Department of Electrical Engineering and Computer Science, Research Laboratory of Electronics, Massachusetts Institute of Technology, Cambridge, MA, USA

Abstract

Purpose: The appearance and growth of persistent choroidal hypertransmission defects (hyperTDs) detected on *en face* swept-source OCT (SS-OCT) images from eyes with intermediate AMD (iAMD) were studied to determine if they could serve as novel clinical trial endpoints.

Design: Post-hoc subgroup analysis of a prospective study.

Methods: Subjects with iAMD underwent 6 x 6 mm SS-OCT angiography (SS-OCTA) imaging at their baseline and follow-up visits. The drusen volumes were obtained using a validated SS-OCT algorithm. Two graders independently evaluated all *en face* structural images for the presence of persistent hyperTDs. The number and area of all hyperTDs along with drusen

Corresponding Author: Philip J. Rosenfeld MD, PhD, Bascom Palmer Eye Institute, 900 NW 17th Street, Miami, FL 33136, Phone: 305-326-6148, Fax: 305-326-6538, prosenfeld@miami.edu.

Financial Disclosures: Giovanni Gregori and Philip J. Rosenfeld received research support from Carl Zeiss Meditec, Inc. Giovanni Gregori and the University of Miami coown a patent that is licensed to Carl Zeiss Meditec, Inc. Dr. Rosenfeld also received research funding from Alexion Pharmaceuticals, Gyroscope Therapeutics, and Stealth BioTherapeutics. He is also a consultant for Annexon, Apellis, Boehringer-Ingelheim, Carl Zeiss Meditec, Chengdu Kanghong Biotech, Ocunexus Therapeutics, Ocudyne, Regeneron Pharmaceuticals, and Unity Biotechnology. He also has equity interest in Apellis, Valitor, Verana Health, and Ocudyne. Nadia K. Waheed is Chief Medical Officer at AGTC and receives research support from Carl Zeiss Meditec, Nidek and Topcon. She has received speaker fees from Nidek. She has an equity interest in Ocudyne, and is a consultant for Olix Therapeutics, Stealth, Complement Therapeutics, Hubble, Topcon, Saliogen, and Syncona. Eric M. Moult and James G. Fujimoto have a patent with a license option to Topcon Healthcare. James G. Fujimoto receives research support from Topcon Healthcare. He has equity interest in Optovue and receives royalties on a patent owned by MIT and licensed to Optovue. He receives speaker fees from the Bascom Palmer Eye Institute. The remaining authors have no disclosures.

volume were obtained from all SS-OCTA scans. Eyes were censored from further follow-up once exudative AMD developed.

Results: A total of 171 eyes from 121 patients with iAMD were included. Sixty-eight eyes developed at least one hyperTD. Within one year after developing a hyperTD, 25% of eyes developed new hyperTDs for an average of 0.44 additional hyperTDs. Over two years, as hyperTDs appeared, enlarged, and merged, the average area growth rate was 0.220 mm/yr using the square-root transformation strategy. A clinical trial design utilizing the onset and enlargement of these hyperTDs for the study of disease progression in eyes with iAMD is proposed.

Conclusions: The appearance and growth of persistent choroidal hyperTDs in eyes with iAMD can be easily detected and measured using *en face* OCT imaging and can serve as novel clinical trial endpoints for the study of therapies that may slow disease progression from iAMD to late AMD.

Graphical Abstract

The onset and progression of persistent choroidal hypertransmission defects (hyperTDs) detected with *en face* OCT imaging of eyes with intermediate AMD (iAMD) demonstrates how geographic atrophy begins by the formation of these focal defects, which grow and coalesce over time. The initial development and growth of these hyperTDs can serve as a novel clinical trial endpoint for testing therapies that may slow disease progression from iAMD to late AMD.

INTRODUCTION

Age-related macular degeneration (AMD), a leading cause of irreversible vision loss and blindness among the elderly worldwide,[1] has been classified into three progressive stages using color fundus (CF) imaging.[2] These stages are referred to as early, intermediate, and late AMD. Early AMD is defined by the presence of numerous small (diameter < 63 μm) or medium size drusen (diameter ≥ 63 μm but < 125 μm). Intermediate AMD (iAMD) is characterized by the appearance of at least one large druse (diameter ≥ 125 μm) or a medium size druse with the presence of pigmentary abnormalities. Finally, late AMD is characterized by the presence of exudative macular neovascularization (MNV) or geographic atrophy (GA), also known as complete retinal pigment epithelium and outer retinal atrophy (cRORA).[3,4] While these stages of disease progression are based on the use of CF imaging, other imaging modalities such as fundus autofluorescence (FAF), near-infrared reflectance (NIR), and optical coherence tomography (OCT) imaging have recently taken on more prominent roles in clinical practice and clinical trials.[4] However, for the detection and characterization of macular atrophy in AMD, the Classification of Atrophy Meeting (CAM) group developed a consensus recommendation that OCT should be the preferred imaging strategy.[3,4] This CAM consensus report relied primarily on the use of averaged individual B-scans for the grading of macular atrophy. Another promising OCT strategy shown to be useful for the detection of macular atrophy in AMD is *en face* OCT imaging using closely spaced raster B-scans.[5-9] One of the advantages of *en face* OCT imaging is its ability to use all the information contained within the raster scan volume to provide a three-dimensional view of the disease. This is achieved by combining cross-sectional imaging from B-scans with *en face* images generated using boundary specific segmentations. The *en face* OCT

imaging strategy is similar to viewing the fundus on color, NIR, and FAF images with the added value of B-scan depth information. This enables the detection of atrophy at a single glance, without having to scroll through the entire volume of individual B-scans.

Both spectral domain (SD) and swept-source (SS) OCT imaging can be used to generate *en face* images derived from closely spaced cross-sectional B-scans. OCT angiography (OCTA) uses a dense raster of repeated B-scans to generate vasculature contrast in addition to structural information. Acquiring OCTA at every stage of AMD can detect and measure drusen area and volume,[10] the presence of persistent choroidal hypertransmission defects (hyperTDs) and cRORA,[5-9] the extent of hyperpigmentation,[11] the presence of calcified drusen,[12] the presence of nonexudative MNV,[13,14] and the presence of exudation that arises from MNV.[15] All of this information can be acquired from the same OCTA scan pattern. An especially important advantage of using *en face* OCTA imaging in iAMD is its ability to identify the initial appearance and subsequent growth of persistent choroidal hyperTDs, which are defined as bright regions having a greatest linear dimension (GLD) that is ≥ 250 μm in any *en face* direction. The hyperTD appears bright compared to the surrounding area on the *en face* image due to the increased light transmission into the choroid where the retinal pigment epithelium (RPE) is absent or attenuated. Of note, bright regions with a GLD < 250 μm were more likely to be transient.[16] These persistent hyperTDs are similar to cRORA lesions. However, cRORA lesions are defined only on horizontal B-scans.[9] It is also important to appreciate that persistent hyperTDs might correspond to lesions that would be classified as incomplete RORA (iRORA) on individual horizontal B-scans, but might measure 250 μm or greater in another transverse dimension using *en face* OCT imaging. This calls into question the validity of using individual B-scans rather than assessing multiple closely spaced adjacent B-scans to distinguish between iRORA and cRORA.[4,7,17] To demonstrate that clinicians and graders can easily detect persistent choroidal hyperTDs using *en face* OCT imaging, we performed an exercise in which graders were trained to diagnose hyperTD lesions and then were given a test-set of cases. Overall, the graders detected these lesions with high sensitivity, accuracy, positive predictive value, and intergrader agreement.[7]

Another advantage of using *en face* imaging in eyes with iAMD is that the appearance of persistent hyperTDs can be detected and their enlargement rates measured in a manner that is similar to how GA growth is measured using FAF, NIR, and other *en face* imaging modalities. By contrast, using individual horizontal B-scans to detect the appearance and growth of cRORA only measures changes in the horizontal (nasal-temporal) direction, and the B-scan must be positioned over the hyperTD when it first appears and reproducibly positioned on follow-up examinations. We found that *en face* OCT imaging can reliably detect the appearance and measure the two-dimensional growth of hyperTDs once an eye develops its first atrophic lesion. With the goal of using *en face* imaging to characterize disease progression in eyes with iAMD, we designed a protocol to study the appearance and growth of persistent hyperTDs.

In this report, we present our protocol using the 6 x 6 mm volumetric SS-OCTA scans to measure the progression of drusen volume over time and to detect the onset and growth of persistent hyperTDs in eyes with iAMD. Based on these observations, we propose a novel

clinical trial design that detects the onset and growth of persistent hyperTDs that can be used as clinical trial endpoints for studies investigating novel therapies that may slow the progression of iAMD to late AMD.

METHODS

Patients with AMD were enrolled in a prospective, observational, SS-OCT imaging study at the Bascom Palmer Eye Institute. The institutional review board of the University of Miami Miller School of Medicine approved the study, and all patients signed an informed consent for this prospective SS-OCT study. The study was performed in accordance with the tenets of the Declaration of Helsinki and complied with the Health Insurance Portability and Accountability Act of 1996.

Participants

A post-hoc retrospective review of this prospective observational SS-OCT imaging study included eyes from patients followed from April 2016 to May 2022. Patients did not receive any active therapy in the study eye and all of them had the diagnosis of iAMD defined by the presence of at least one large druse with a minimal diameter of 125 μm (equivalent to an approximate minimal volume of 0.001 mm^3) in a 5 mm circle centered on the fovea. To be included in this study, patients had to have at least one-year of follow-up between their baseline visit, when they qualified for this retrospective review study, and their last available follow-up visit. Exclusion criteria at baseline included a history of exudative MNV, a persistent hyperTD, cRORA (GA), diabetic retinopathy, or any concomitant retinal disease associated with drusen-like deposits, such as Stargardt disease or vitelliform dystrophy. In addition, patients were excluded if their eyes contained any vitreoretinal interface disease that caused marked distortion of the macular anatomy.

Imaging Protocols

All eyes underwent SS-OCT imaging (PLEX® Elite 9000, Carl Zeiss Meditec, Dublin, CA) at baseline and during follow-up visits, and scans were acquired by one of two trained imaging technicians. The SS-OCT light source had a central wavelength of 1050 nm and a bandwidth of 100 nm, corresponding to a full width at half-maximum axial resolution in tissue of approximately 5 μm. The transverse optical resolution at the retinal surface was approximately 20 μm. The instrument operated at a scanning speed of 100,000 A-scans per second. All patients were imaged using the SS-OCT angiography (SS-OCTA) 6 x 6 mm scan pattern centered on the fovea. This scan pattern consisted of 500 A-scans per B-scan, with each B-scan repeated twice at each position to generate the angiographic signal, and 500 B-scan positions along the perpendicular slow scan axis, resulting in a uniform spacing of 12 μm between A-scans. Each A-scan spanned a depth of 3 mm consisting of 1536 pixels per A-scan. The angiographic contrast was obtained using the complex optical microangiographic algorithm known as $OMAG^C$ that generates flow signals from variations in both OCT signal magnitude and phase between repeated B-scans acquired at the same position.[18,19] Each volumetric data set was reviewed for quality and signal strength, and scan with a signal strength less than 7 based on the instrument's output, as well as those with significant motion artifacts were excluded. If more than one scan of a given type was

available at a visit, the best quality data was chosen. The drusen volume (mm^3) and RPE elevation maps were generated and validated using the Advanced RPE Analysis Algorithm version 0.10 (Carl Zeiss Meditec, USA) as described by Jiang *et al.*[10]

All eyes were screened for the presence of non-exudative MNV by using two SS-OCTA *en face* slabs. One slab extended from the outer retina to the choriocapillaris, known as the ORCC slab that was used primarily as an overview to detect all types of MNV. Evidence of non-exudative type 3 MNV was obtained by reviewing the *en face* ORCC slab and the OCTA cross-sectional B-scans, especially in suspicious areas with increased retinal thickening. The second slab extended from the RPE to Bruch's membrane (BM), and this slab was used primarily to detect type 1 MNV. In addition, corresponding structural and OCTA B-scans were used to further identify low-lying irregular RPE elevations consistent with the presence of non-exudative type 1 MNV. All images were reviewed to assess for evidence of exudation, which was defined as the appearance of any subretinal or intraretinal fluid on structural OCT B-scans and on the retinal thickness maps.

Grading of Persistent Choroidal HyperTDs

Persistent hyperTDs were identified as areas of increased focal brightness, corresponding to the hypertransmission of light into the choroid, measuring at least 250 μm in GLD. These persistent choroidal hyperTDs were detected by using an *en face* image from a sub-RPE slab positioned from 64 to 400 μm beneath BM, as previously reported.[7,9,16] Two independent graders (J.L., M.S.) evaluated all the *en face* images for the presence of these lesions in the eyes with iAMD that only had drusen at baseline. Once identified in a follow-up visit, the graders measured the GLD for each hyperTD using the software caliper from the instrument. Multiple hyperTDs could be identified in an eye at a follow-up visit. After hyperTDs ≥ 250 μm were identified on the *en face* sub-RPE OCT slabs, B-scans through the lesions were reviewed to confirm the presence of hyperTDs. The two graders tried to reach a consensus agreement for the manual outlines of each lesion, and any remaining disagreement was adjudicated by a senior grader (P.J.R.). The area measurements for each of the hyperTD lesions were obtained by using a proprietary, validated algorithm that identified and measured the areas of each persistent hyperTD.[20] Any discrepancy between the outlines of the hyperTD lesions from the automated algorithm and manual outlines was adjusted in the algorithm using a built-in editing tool. For each eye, all the available visits were reviewed and annotated for the development of the first persistent hyperTD with a GLD ≥ 250 μm and for all subsequent persistent hyperTDs. After they were identified, each hyperTD was labelled with a unique number, and they were followed over time as the lesions enlarged and merged into larger persistent choroidal hyperTDs (Figure 1). Eyes were also graded for the formation of exudative MNV and after symptomatic exudation was detected and treated with intravitreal injections of a vascular endothelial growth factor (VEGF) inhibitor, these eyes were no longer followed in this natural history study.

After the first persistent hyperTD was identified in each eye, additional persistent hyperTDs soon developed, and their growth and convergence to form larger hyperTDs were tracked. The areas of the hyperTDs were measured at each visit, and their growth characteristics

were studied by using the square-root transformation strategy for the total area of the hyperTDs.[21]

To validate the growth characteristics of small, persistent hyperTDs that formed in the primary dataset consisting of eyes with iAMD that started with only drusen at baseline, a secondary independent dataset of eyes with small hyperTDs having a total area of ≤ 0.5 disc area or ≤ 1.25 mm^2 at the baseline visit was analyzed. Using the previously described protocol, at least two independent graders (G.H., J.L., Y.S.) evaluated each of the *en face* images and measured the GLD for each hyperTD. The graders reached a consensus agreement for the manual outlines of each lesion, and any remaining disagreement was adjudicated by a senior grader (P.J.R.). The area measurements for each of the hyperTD lesions was obtained by using the algorithm previously mentioned.[20] Any discrepancy between the outlines of the hyperTD lesions from the automated algorithm and manual outlines were adjusted in the algorithm using the built-in editing tool.

Statistical Analysis

Kaplan-Meier survival methods were used to summarize the initial onset and appearance of additional persistent choroidal hyperTDs. Data were censored at the last available visit date or when exudation occurred. For hyperTD area measurements, the square-root transformation (mm) was used while drusen volume was measured in mm^3. The influence of drusen volume on the incidence and growth rate of hyperTDs were investigated by mixed-effect models, accounting for the within-eye and within-subject correlations among the longitudinal data. The receiver operating characteristic (ROC) approach was applied on drusen volume to guide the selection of an enhanced study population with a higher likelihood of developing persistent hyperTDs in a year. Statistical analyses were performed with SAS Version 9.4 (SAS Institute, Cary, NC) with a p-value of < 0.05 being considered statistically significant.

RESULTS

Baseline Characteristics

A total of 171 eyes with only drusen at baseline from 121 patients with iAMD in at least one eye were enrolled. Of the 121 patients, the mean age was 74.0 ± 7.3 years and 64% were women. The follow-up intervals were variable since most patients were imaged as part of their routine clinical care. Eyes were followed for a mean of 43 ± 16.5 months (median: 42.7; range 12.0 to 72.0), with 89% of eyes being followed for at least 24 months, 64% for at least 36 months, and 37% for at least 48 months. The average number of follow-up visits per year was one for 20% of eyes, between 2 and 3 for 48% of eyes, and ≥ four for 32% of eyes. Fifteen eyes (8.8%) from 13 patients (10.7%) developed exudative AMD during the study period and were censored after exudation was detected.

Prevalence of Persistent Choroidal HyperTDs

By the time of the last available follow-up visit at 72 months, 68 eyes (39.8%) had developed at least one persistent hyperTD. Figure 2 shows an example of how multiple hyperTDs formed, enlarged, and merged over time. Figure 3A shows the Kaplan-Meier

cumulative proportion of iAMD eyes that developed at least one hyperTD over time. By one year, 10% of eyes had developed at least one persistent hyperTD. After the first hyperTD was detected, 27 eyes (15.8%) developed additional hyperTDs. Figure 3B shows the Kaplan-Meier cumulative proportion of iAMD eyes that developed additional hyperTDs after the detection of the first lesion. The median time to develop an additional hyperTD was 19.7 months (95%CI: 15.6 to 27.9). Within a year after developing a hyperTD, 25% of eyes developed new hyperTDs for an average of 0.44 additional hyperTDs.

Growth Characteristics of Persistent Choroidal HyperTDs

Of the 68 eyes that developed hyperTDs, 55 eyes from 51 patients had additional follow-up after the onset of a hyperTD (for at least 1 year in 50 eyes, at least 2 years in 23 eyes, and at least 3 years in 13 eyes). The mean baseline hyperTD area using the square root transformation was 0.389 ± 0.207 mm (median: 0.30; range: 0.22 to 1.45). From our observations, one to several small hyperTDs would develop on the *en face* OCT image. Over time, these hyperTDs would gradually enlarge and new hyperTDs would emerge. Eventually, individual hyperTDs would merge together to form one or more larger areas of atrophy that would gradually encompass the macula. Examples of this progression is shown in Figures 2 and 4. These figures show eyes starting with only drusen at baseline that developed multiple hyperTDs over time that grow and merge together to form larger areas of GA. Using the square-root transformation strategy, we found that the average area growth rates over 1 and 2 years since the onset of a hyperTD were 0.266 ± 0.289 mm/yr and 0.220 ± 0.200 mm/yr, respectively.

As previously mentioned, to validate the growth characteristics of hyperTDs that formed in the primary dataset consisting of eyes with iAMD that started with only drusen at baseline, a second independent dataset of eyes was analyzed that contained small hyperTDs having a total area measurement of ≤ 0.5 disc area or ≤ 1.25 mm^2 at their baseline visit. This supplemental dataset contained 59 eyes from 50 patients. The baseline hyperTD area using the square-root transformation was 0.583 ± 0.262 mm (median 0.52; range: 0.23 to 1.12). The average growth rates over 1 and 2 years were 0.267 ± 0.300 mm/yr and 0.221 ± 0.207 mm/yr, respectively. These rates are very similar to the primary dataset containing hyperTDs that formed from eyes with only drusen at the baseline visit.

Drusen Volume as a Risk Factor for Persistent Choroidal HyperTD Development

Drusen volume was explored as a risk factor for the formation of persistent hyperTDs. The average baseline drusen volume within the 3 mm and 5 mm circles centered on the fovea for all eyes were 0.141 ± 0.173 mm^3 and 0.169 ± 0.204 mm^3, respectively. The average baseline drusen volume within the 3 mm and 5 mm circles for eyes that developed hyperTDs were 0.201 ± 0.212 mm^3 and 0.249 ± 0.249 mm^3, respectively. The average drusen volumes within the 3 mm and 5 mm circles at the last visit prior to the appearance of a hyperTD were 0.263 ± 0.356 mm^3 and 0.332 ± 0.405 mm^3. In contrast, the average baseline drusen volumes within the 3 mm and 5 mm circles for eyes that did not develop hyperTDs were 0.101 ± 0.131 mm^3 and 0.114 ± 0.150 mm^3, respectively. The average drusen volumes within the 3 mm and 5 mm circles at the last visit of eyes that did not develop hyperTDs were 0.161 ± 0.179 mm^3 and 0.189 ± 0.212 mm^3, respectively.

In both the 3 mm and 5 mm circles, the eyes that developed hyperTDs had a significantly higher drusen volume at baseline ($p = 0.0014$ and $p = 0.0004$, respectively) and at the last visit prior to the onset of a hyperTD ($p = 0.025$ and $p = 0.008$, respectively) compared with eyes that did not develop a hyperTD at the last visit.

Clinical Trial Design Using Drusen Volume and Persistent Choroidal HyperTD Growth Rate

Based on the above results, a clinical trial can be designed that enrolls patients that are likely to develop hyperTDs using drusen volume as a risk factor. We used the drusen volume within a 5 mm circle centered on the fovea since early hyperTDs could be found to develop outside the 3 mm circle, but within the 5 mm circle. Moreover, the algorithm that determined drusen volume showed greater reproducibility with the 5 mm circle since it was less dependent on the precise automated localization of the foveal center.[10] Figure 5 shows the ROC curve used to find the best drusen volume cutoff for an eye that is likely to develop a hyperTD within 12 months. The drusen volume within a 5 mm circle centered on the fovea at 9 to 15 months prior to the onset of hyperTDs or the censored timepoint comprised the analysis dataset for the ROC. The drusen volume nearest to 12 months was used if there were multiple visits within 9 to 15 months. The average drusen volume within the 5 mm circle at one year preceding the formation of the first hyperTD was approximately 0.18 mm^3. From the ROC plot, a drusen volume ≥ 0.20 mm^3 or ≥ 0.25 mm^3 within the 5 mm circle centered on the fovea would predict that about 58.3% or 68.2% of cases starting with only drusen at baseline would develop a hyperTD within one year, respectively.

Table 1 shows the sample sizes needed in each arm of a clinical study at a given power and statistical significance to show a reduction of the hyperTD growth rate by 50%, 40%, 30%, and 20% based on the natural history growth rate of small persistent hyperTDs. Prior to following the growth of hyperTDs, Table 2 shows the baseline number of subjects with iAMD and a minimum drusen volume in at least one eye that is needed to have the required number of subjects that will develop at least one hyperTD by one-year of follow-up. These subjects with hyperTDs can then be followed in the second year of the study to determine if a given therapy slows the growth rate of hyperTDs by a given percentage over that second year. Based on these tables, if we want to run a two-year study that has an 80% power at a significant alpha level of 0.05 to detect a treatment effect that slows the growth rate by 50% (control growth rate: 0.220 mm/yr) when hyperTDs first appear, we need to enroll at least 91 subjects per group with baseline drusen volumes ≥ 0.20 mm^3 in at least one eye. This will allow us to have at least 53 subjects per group to follow the growth of the hyperTDs in the second year of the study.

DISCUSSION

In this study, we analyzed the onset and growth of persistent hyperTDs using *en face* SS-OCT images of eyes with iAMD. About 40% of eyes developed at least one hyperTD over the study period. After the hyperTDs formed, the average area growth rate over 2 years was 0.220 mm/yr. This growth rate was determined from eyes with only drusen at baseline that developed hyperTDs during the study period and was confirmed in a secondary sample of eyes that already had small hyperTDs at baseline. Our growth rates are slower

than previous reports investigating the growth of GA in eyes with late AMD using *en face* OCT, CF, or FAF imaging.[16,21-33] The growth rates for those studies using the square root transformation strategy ranged from 0.27 to 0.40 mm/yr. However, these previous studies had a mean baseline GA size of at least 2.20 mm^2, with the majority of them having a mean baseline GA size of > 7.00 mm^2.[22] This is significantly larger than our mean baseline hyperTD area of about 0.19 mm^2 (square root transformation: 0.389 mm). Thus, these previous studies were analyzing lesions that were considerably more advanced than those in our study. In addition, many of the previous studies used either CF or FAF imaging to measure GA area in contrast to our study using *en face* OCT imaging.[22] Also, to validate the growth rate of hyperTDs developing from eyes with only drusen at baseline, we analyzed a second independent sample of eyes beginning with small hyperTDs at the baseline visit. The average growth rate over 2 years in this secondary sample was 0.221 mm/yr, which is very close to the rates from the primary dataset with iAMD eyes starting with only drusen. Thus, to the best of our knowledge, this is the first study to investigate the onset and growth of small persistent hyperTDs in eyes with iAMD as they progress into larger areas of GA or cRORA.

From our observations, small persistent hyperTDs appear as bright areas on the *en face* OCT image measuring at least 250 μm in GLD. They usually develop in areas preceded by either soft or calcified drusen and/or hyperpigmentation, which appear as dark foci on the *en face* OCT image, known as hypotransmission defects (hypoTDs).[11,12] Over time, these hyperTDs would enlarge and new lesions would appear, grow, and merge with the original lesion. Eventually, as multiple hyperTDs grow and coalesce, a larger area of typical GA or cRORA becomes apparent (Figures 2 and 4). One advantage of using *en face* OCT imaging is its ability to use the same volumetric dataset to assess drusen volume, the appearance of hyperTDs, and the growth of these lesions in any *en face* transverse dimension versus individual B-scans which can only assess changes in the horizontal direction.[7] For B-scan assessment to approach the sensitivity of *en face* imaging, the B-scans need to be closely spaced as in our current SS-OCTA raster scan pattern. It is noteworthy that the scan pattern used in this study had 500 horizontal B-scans in a 6 x 6 mm raster scan pattern, which corresponds to a spacing of 12 μm between B-scans. Since the growth of atrophic lesions do not necessarily occur along the horizontal meridian, the use of dense B-scans to generate these *en face* images provides a powerful strategy for the detection and measurement of hyperTDs as shown in Figures 2 and 4. In addition, *en face* imaging provides an easier and faster strategy for identifying and measuring hyperTDs compared with previous strategies that require tedious examination of every B-scan to identify nascent GA, iRORA, and cRORA.[3,17,34,35] As a result, *en face* OCT imaging provides an accurate and convenient method to monitor the onset and progression of persistent hyperTDs, a precursor lesion to typical GA.[9]

In addition to investigating the onset and progression of hyperTDs, drusen volume was explored as a risk factor for the formation of these lesions. As previously mentioned, the eyes that developed hyperTDs had a significantly greater drusen volume at baseline and at the last visit prior to the onset of a hyperTD compared with eyes that did not develop a hyperTD during the study period. This is consistent with a study by Abdelfattah et al.[36], which showed that eyes that developed late AMD had a significantly larger baseline drusen

volume than eyes that did not progress, which is also supported by other studies.[37-39] In addition, Abdelfattah et al.[36] reported that eyes with a drusen volume > 0.03 mm^3 had a greater than 4-fold increased risk for developing late AMD compared to those with lower drusen volumes. We originally identified this drusen volume of > 0.03 mm^3 in an earlier study that we performed to investigate if a systemic complement inhibitor could slow drusen growth and perhaps even decrease the drusen volume by 50%.[40] We chose this drusen volume as a mid-range value that could be reliably followed to determine if there was an increase or decrease in drusen volume and not as a predictor of disease progression. Thus, it is not surprising that a drusen volume to identify eyes that will likely develop hyperTDs within one year of enrollment would be larger than the mid-range drusen volume previously studied. Furthermore, it was reassuring that the average baseline drusen volume within the 5 mm circle for eyes that did not form hyperTDs was 0.114 mm^3, which was less than the drusen volume of ≥ 0.20 mm^3 identified on the ROC plot to predict the formation of hyperTDs within 12 months (Figure 5). Also, other risk factors such as hyperpigmentation and calcified drusen are likely to serve as important predictors of disease progression to hyperTDs[39,41] and are currently being investigated in ongoing studies using the same SS-OCT scan patterns.

We intended to use this natural history study to design a clinical trial to test therapies that may slow disease progression from iAMD to late AMD, with a focus on the formation and growth of hyperTDs. The primary objectives of such a clinical trial would be to enroll patients with iAMD at high risk of disease progression and then randomize these subjects into active treatment and placebo. This study has two primary endpoints that not only involve the formation of hyperTDs, but also a slowing of their enlargement once they develop. Since it may be impossible to prevent the formation of any hyperTDs in these high-risk eyes, the benefit of our clinical trial design is that we will be able to determine if a potential therapy not only slows the formation of these hyperTDs but also slows their enlargement. Therefore, the study is designed in two phases. The first phase aims to enroll high risk iAMD eyes that are likely to develop hyperTDs within one year. This will allow a sufficient number of eyes that develop a hyperTD to be included in the second phase of the study that will involve following these eyes in the second year to determine if a potential therapy slows the enlargement of the hyperTDs. This novel clinical trial design satisfies the requirement of regulatory bodies that want a randomized trial to demonstrate if a potential therapy slows disease progression while being able to enroll eyes without any evidence of late stage AMD, since these late stage eyes with nonexudative AMD may be candidates for treatment with emerging novel therapies that may be approved to prevent the enlargement of GA.[32,42] In our clinical trial design, we plan to enroll at least 91 subjects per group with drusen volumes ≥ 0.20 mm^3 in at least one eye at baseline. This will allow us to have approximately 53 subjects per group to follow in the second year, so that with an assumed hyperTD growth rate of 0.220 mm/yr for the control, we will have an 80% power to detect a 50% slowing of hyperTD growth with a significant alpha level of 0.05 (Tables 1 and 2).

A strength of our study includes our use of a novel, accurate, and reproducible imaging method along with a unique study design to monitor the formation and growth of hyperTDs in eyes with drusen. To the best of our knowledge, this is the first report utilizing *en face* SS-OCT imaging to investigate the onset and progression of persistent hyperTDs in

eyes with iAMD starting with only drusen at baseline. In addition, the use of a secondary independent dataset to validate the growth rate of the hyperTDs strengthens our findings. Finally, the results from this report are applicable to design a clinical trial to prevent the formation and progression of persistent hyperTDs in eyes with iAMD.

Limitations of this study include the use of *en face* SS-OCT images from a specific instrument that generated dense volumetric scans and is not yet widely available. However, the availability of SS-OCT is growing and the more accessible SD-OCT instruments are capable of producing *en face* images that can be used to detect and monitor hyperTDs.[16,43,44] In addition, other risk factors, such as hyperpigmentation and calcified drusen, are likely to serve as predictors of disease progression, but were not included in this study. In the future, the addition of these risk factors should enable a broader recruitment of subjects into a clinical trial that may not meet the drusen volume criterion for enrollment.

In conclusion, this study describes the use of *en face* SS-OCT imaging to detect the formation and growth of persistent choroidal hyperTDs in eyes with iAMD. In addition, it provides natural history data on hyperTD formation based on drusen volume and their rate of enlargement as these lesions grow. Together, the onset and progression of persistent hyperTDs can serve as novel clinical trial endpoints for the study of therapies that may slow disease progression from iAMD to late AMD.

Funding/Support:

Research supported by grants from Carl Zeiss Meditec, Inc. (Dublin, CA), the Salah Foundation, the National Eye Institute Center Core Grant (P30EY014801 and R01-EY011289-36) and Research to Prevent Blindness (unrestricted Grant) to the Department of Ophthalmology, University of Miami Miller School of Medicine. The funding organization had no role in the design or conduct of this research.

Other Acknowledgements:

In memory of our beloved colleague, William J. Feuer, an extraordinary biostatistician and scientist who initiated the statistical analyses for this manuscript. We also appreciate the exceptional technical expertise of Linda O'Koren and Mark Lazcano in obtaining all the SS-OCT scans.

REFERENCES

1. Fleckenstein M, Keenan TDL, Guymer RH, et al. Age-related macular degeneration. Nat Rev Dis Primers. 2021;7(1):31. [PubMed: 33958600]
2. Ferris FL 3rd, Wilkinson CP, Bird A, et al. Clinical classification of age-related macular degeneration. Ophthalmology. 2013;120(4):844–851. [PubMed: 23332590]
3. Sadda SR, Guymer R, Holz FG, et al. Consensus Definition for Atrophy Associated with Age-Related Macular Degeneration on OCT: Classification of Atrophy Report 3. Ophthalmology. 2018;125(4):537–548. [PubMed: 29103793]
4. Jaffe GJ, Chakravarthy U, Freund KB, et al. Imaging Features Associated with Progression to Geographic Atrophy in Age-Related Macular Degeneration: Classification of Atrophy Meeting Report 5. Ophthalmol Retina. 2021;5(9):855–867. [PubMed: 33348085]
5. Yehoshua Z, de Amorim Garcia Filho CA, Nunes RP, et al. Comparison of Geographic Atrophy Growth Rates Using Different Imaging Modalities in the COMPLETE Study. Ophthalmic Surg Lasers Imaging Retina. 2015;46(4):413–422. [PubMed: 25970861]
6. Shi Y, Zhang Q, Zhou H, et al. Correlations Between Choriocapillaris and Choroidal Measurements and the Growth of Geographic Atrophy Using Swept Source OCTImaging. Am J Ophthalmol. 2020;224:321–331. [PubMed: 33359715]

7. Liu J, Laiginhas R, Corvi F, et al. Diagnosing Persistent Hypertransmission Defects on En Face OCT Imaging of Age-Related Macular Degeneration. Ophthalmol Retina. 2022;6(5):387–397. [PubMed: 35093585]
8. Velaga SB, Nittala MG, Hariri A, Sadda SR. Correlation between Fundus Autofluorescence and En Face OCT Measurements of Geographic Atrophy. Ophthalmol Retina. 2022;6(8):676–683. [PubMed: 35338026]
9. Laiginhas R, Shi Y, Shen M, et al. Persistent Hypertransmission Defects Detected on En Face Swept Source Optical Computed Tomography Images Predict the Formation of Geographic Atrophy in Age-Related Macular Degeneration. Am J Ophthalmol. 2022;237:58–70. [PubMed: 34785169]
10. Jiang X, Shen M, Wang L, et al. Validation of a Novel Automated Algorithm to Measure Drusen Volume and Area Using Swept Source Optical Coherence Tomography Angiography. Transl Vis Sci Technol. 2021;10(4):11.
11. Laiginhas R, Liu J, Shen M, et al. Multimodal Imaging, OCT B-Scan Localization, and En Face OCT Detection of Macular Hyperpigmentation in Eyes with Intermediate Age-Related Macular Degeneration. Ophthalmology Science. 2022;2(2):100116. [PubMed: 36249700]
12. Liu J, Laiginhas R, Shen M, et al. Multimodal Imaging and En Face OCT Detection of Calcified Drusen in Eyes with Age-Related Macular Degeneration. Ophthalmol Sci. 2022;2(2).
13. de Oliveira Dias JR, Zhang Q, Garcia JMB, et al. Natural History of Subclinical Neovascularization in Nonexudative Age-Related Macular Degeneration Using Swept-Source OCT Angiography. Ophthalmology. 2018;125(2):255–266. [PubMed: 28964581]
14. Yang J, Zhang Q, Motulsky EH, et al. Two-Year Risk of Exudation in Eyes with Nonexudative Age-Related Macular Degeneration and Subclinical Neovascularization Detected with Swept Source Optical Coherence Tomography Angiography. Am J Ophthalmol. 2019;208:1–11. [PubMed: 31229464]
15. Shen M, Rosenfeld PJ, Gregori G, Wang RK. Predicting the Onset of Exudation in Treatment-Naive Eyes with Nonexudative Age-Related Macular Degeneration. Ophthalmol Retina. 2022;6(1):1–3. [PubMed: 34996537]
16. Shi Y, Yang J, Feuer W, Gregori G, Rosenfeld PJ. Persistent Hypertransmission Defects on En Face OCT Imaging as a Stand-Alone Precursor for the Future Formation of Geographic Atrophy. Ophthalmol Retina. 2021.
17. Guymer RH, Rosenfeld PJ, Curcio CA, et al. Incomplete Retinal Pigment Epithelial and Outer Retinal Atrophy in Age-Related Macular Degeneration: Classification of Atrophy Meeting Report 4. Ophthalmology. 2020;127(3):394–409. [PubMed: 31708275]
18. Wang RK, An L, Francis P, Wilson DJ. Depth-resolved imaging of capillary networks in retina and choroid using ultrahigh sensitive optical microangiography. Opt Lett. 2010;35(9):1467–1469. [PubMed: 20436605]
19. Zhang A, Zhang Q, Chen CL, Wang RK. Methods and algorithms for optical coherence tomography-based angiography: a review and comparison. J Biomed Opt. 2015;20(10):100901. [PubMed: 26473588]
20. Chu Z, Shi Y, Zhou X, et al. Optical Coherence Tomography Measurements of the Retinal Pigment Epithelium to Bruch Membrane Thickness Around Geographic Atrophy Correlate With Growth. Am J Ophthalmol. 2022;236:249–260. [PubMed: 34780802]
21. Yehoshua Z, Rosenfeld PJ, Gregori G, et al. Progression of geographic atrophy in age-related macular degeneration imaged with spectral domain optical coherence tomography. Ophthalmology. 2011;118(4):679–686. [PubMed: 21035861]
22. Wang J, Ying GS. Growth Rate of Geographic Atrophy Secondary to Age-Related Macular Degeneration: A Meta-Analysis of Natural History Studies and Implications for Designing Future Trials. Ophthalmic Res. 2021;64(2):205–215. [PubMed: 32721951]
23. Grunwald JE, Pistilli M, Daniel E, et al. Incidence and Growth of Geographic Atrophy during 5 Years of Comparison of Age-Related Macular Degeneration Treatments Trials. Ophthalmology. 2017;124(1):97–104. [PubMed: 28079023]
24. Monés J, Biarnés M. The Rate of Progression of Geographic Atrophy Decreases With Increasing Baseline Lesion Size Even After the Square Root Transformation. Transl Vis Sci Technol. 2018;7(6):40. [PubMed: 30619660]

25. Nunes RP, Gregori G, Yehoshua Z, et al. Predicting the progression of geographic atrophy in age-related macular degeneration with SD-OCT en face imaging of the outer retina. Ophthalmic Surg Lasers Imaging Retina. 2013;44(4):344–359. [PubMed: 23883530]
26. Stetson PF, Yehoshua Z, Garcia Filho CA, Portella Nunes R, Gregori G, Rosenfeld PJ. OCT minimum intensity as a predictor of geographic atrophy enlargement. Invest Ophthalmol Vis Sci. 2014;55(2):792–800. [PubMed: 24408973]
27. Holekamp N, Wykoff CC, Schmitz-Valckenberg S, et al. Natural History of Geographic Atrophy Secondary to Age-Related Macular Degeneration: Results from the Prospective Proxima A and B Clinical Trials. Ophthalmology. 2020;127(6):769–783. [PubMed: 32081489]
28. Keenan TD, Agrón E, Domalpally A, et al. Progression of Geographic Atrophy in Age-related Macular Degeneration: AREDS2 Report Number 16. Ophthalmology. 2018;125(12):1913–1928. [PubMed: 30060980]
29. Yehoshua Z, de Amorim Garcia Filho CA, Nunes RP, et al. Systemic complement inhibition with eculizumab for geographic atrophy in age-related macular degeneration: the COMPLETE study. Ophthalmology. 2014;121(3):693–701. [PubMed: 24289920]
30. Holz FG, Sadda SR, Busbee B, et al. Efficacy and Safety of Lampalizumab for Geographic Atrophy Due to Age-Related Macular Degeneration: Chroma and Spectri Phase 3 Randomized Clinical Trials. JAMA Ophthalmol. 2018;136(6):666–677. [PubMed: 29801123]
31. Kuppermann BD, Patel SS, Boyer DS, et al. Phase 2 Study of the Safety and Efficacy of Brimonidine Drug Delivery System (BRIMO DDS) Generation 1 in Patients with Geographic Atrophy Secondary to Age-Related Macular Degeneration. Retina. 2021;41(1):144–155. [PubMed: 32134802]
32. Liao DS, Grossi FV, El Mehdi D, et al. Complement C3 Inhibitor Pegcetacoplan for Geographic Atrophy Secondary to Age-Related Macular Degeneration: A Randomized Phase 2 Trial. Ophthalmology. 2020;127(2):186–195. [PubMed: 31474439]
33. Kim BJ, Hunter A, Brucker AJ, et al. Orally Administered Alpha Lipoic Acid as a Treatment for Geographic Atrophy: A Randomized Clinical Trial. Ophthalmol Retina. 2020;4(9):889–898. [PubMed: 32418846]
34. Wu Z, Luu CD, Ayton LN, et al. Optical coherence tomography-defined changes preceding the development of drusen-associated atrophy in age-related macular degeneration. Ophthalmology. 2014;121(12):2415–2422. [PubMed: 25109931]
35. Wu Z, Goh KL, Hodgson LAB, Guymer RH. Incomplete Retinal Pigment Epithelial and Outer Retinal Atrophy: Longitudinal Evaluation in Age-Related Macular Degeneration. Ophthalmology. 2022.
36. Abdelfattah NS, Zhang H, Boyer DS, et al. Drusen Volume as a Predictor of Disease Progression in Patients With Late Age-Related Macular Degeneration in the Fellow Eye. Invest Ophthalmol Vis Sci. 2016;57(4):1839–1846. [PubMed: 27082298]
37. Nassisi M, Lei J, Abdelfattah NS, et al. OCT Risk Factors for Development of Late Age-Related Macular Degeneration in the Fellow Eyes of Patients Enrolled in the HARBOR Study. Ophthalmology. 2019;126(12):1667–1674. [PubMed: 31281056]
38. Folgar FA, Yuan EL, Sevilla MB, et al. Drusen Volume and Retinal Pigment Epithelium Abnormal Thinning Volume Predict 2-Year Progression of Age-Related Macular Degeneration. Ophthalmology. 2016;123(1):39–50.e31. [PubMed: 26578448]
39. Hirabayashi K, Yu HJ, Wakatsuki Y, Marion KM, Wykoff CC, Sadda SR. OCT Risk Factors for Development of Atrophy in Eyes with Intermediate Age-Related Macular Degeneration. Ophthalmol Retina. 2022.
40. Garcia Filho CA, Yehoshua Z, Gregori G, et al. Change in drusen volume as a novel clinical trial endpoint for the study of complement inhibition in age-related macular degeneration. Ophthalmic Surg Lasers Imaging Retina. 2014;45(1):18–31. [PubMed: 24354307]
41. Wu Z, Bogunović H, Asgari R, Schmidt-Erfurth U, Guymer RH. Predicting Progression of Age-Related Macular Degeneration Using OCT and Fundus Photography. Ophthalmol Retina. 2021;5(2): 118–125. [PubMed: 32599175]

42. Jaffe GJ, Westby K, Csaky KG, et al. C5 Inhibitor Avacincaptad Pegol for Geographic Atrophy Due to Age-Related Macular Degeneration: A Randomized Pivotal Phase 2/3 Trial. Ophthalmology. 2021;128(4):576–586. [PubMed: 32882310]

43. Schaal KB, Gregori G, Rosenfeld PJ. En Face Optical Coherence Tomography Imaging for the Detection of Nascent Geographic Atrophy. Am J Ophthalmol. 2017;174:145–154. [PubMed: 27864062]

44. Schaal KB, Rosenfeld PJ, Gregori G, Yehoshua Z, Feuer WJ. Anatomic Clinical Trial Endpoints for Nonexudative Age-Related Macular Degeneration. Ophthalmology. 2016; 123(5): 1060–1079. [PubMed: 26952592]

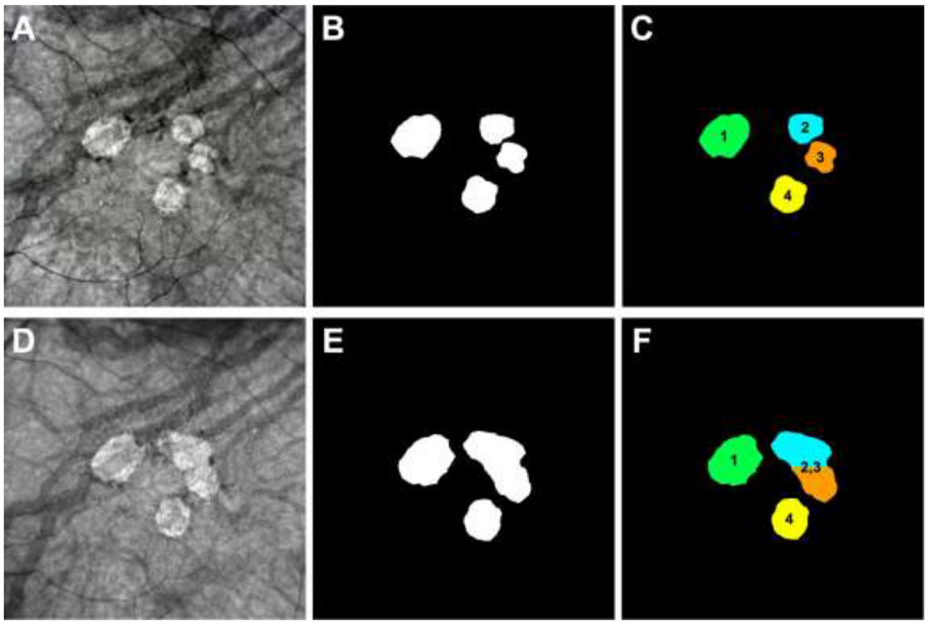

Figure 1:

Detection and monitoring of persistent choroidal hypertransmission defects (hyperTDs) on *en face* swept-source OCT (SS-OCT) structural images from the left eye of an 85-year-old woman with 72 months of follow up. Panels **A-C** represent the 24-month follow-up visit and panels **D-F** represent the 32-month follow-up visit. Panels **A,D** show the *en face* SS-OCT structural images that were created using a slab positioned from 64 to 400 μm under Bruch's membrane. Panels **B,E** show the outlines of the hyperTDs generated by the algorithm and were manually adjusted if needed. Panels **C,F** show how each hyperTD was identified by assigning a unique number to them once a lesion appeared for a given follow-up visit. **(A-C)** At the 24-month follow-up visit, four individual hyperTDs are present on the *en face* SS-OCT image (**A**) with their respective outlines created by the algorithm (**B**). In addition, each lesion is assigned a number based on when the hyperTD was identified in the prior visits (**C**). **(D-F)** At the 32-month follow-up visit, all four lesions enlarge with hyperTDs #2 and #3 merging together (**D,E**). As a result, the merged lesion was labelled hyperTD #2,3 while hyperTD #1 and #4 remained as individual lesions (**F**).

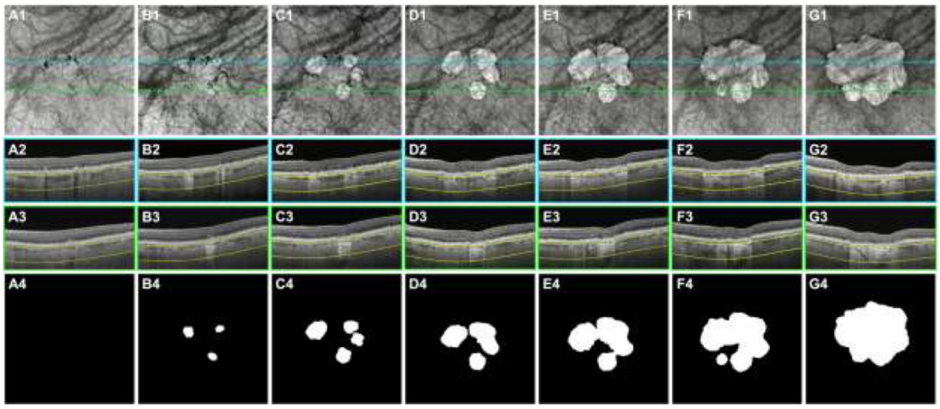

Figure 2:

Swept-source OCT (SS-OCT) imaging of the left eye from an 85-year-old woman beginning with intermediate age-related macular degeneration (iAMD) and progressing to persistent choroidal hypertransmission defects (hyperTDs) over a 72-month period. Column **A** represents the baseline visit, column **B** represents the 16-month follow-up visit, column **C** represents the 24-month follow-up visit, column **D** represents the 36-month follow-up visit, column **E** represents the 48-month follow-up visit, column **F** represents the 57-month follow up visit, and column **G** represents the 72-month follow-up visit. Row **1** shows the *en face* SS-OCT structural images that were created using a slab positioned from 64 to 400 μm under Bruch's membrane. Rows **2** and **3** show the respective B-scans identified by the color-coded lines on the *en face* SS-OCT images. Row **4** shows the outlines of the hyperTDs that were generated by the algorithm and were manually edited if needed. **(A1-A4)** At the baseline visit, hyperpigmentation which are seen as hypotransmission defects (hypoTDs) or dark areas on the *en face* SS-OCT image are present. This is confirmed on the respective B-scan (**A2**) showing intraretinal hyperreflective foci. No hyperTDs are present at this visit (**A1** and **A4**). **(B1-B4)** At the 16-month follow-up visit, three individual hyperTDs are seen on the *en face* SS-OCT image (**B1**) and are confirmed with their respective B-scans showing hypertransmission below the choroid and attenuation of the outer nuclear layer (**B2-B3**). The outlines of the three hyperTDs are shown (**B4**). **(C1-C4)** At the 24-month follow-up visit, the three individual hyperTDs have enlarged with an additional hyperTD appearing on the *en face* SS-OCT image (**C1**). The outlines of the four individual hyperTDs are shown (**C4**). **(D1-D4)** At the 36-month follow-up visit, the hyperTDs continue to enlarge with two of the lesions merging together on the *en face* SS-OCT image (**D1**) and respective outline (**D4**). **(E1-E4)** At the 48-month follow-up visit, all four hyperTDs have grown and merged together to form one large hyperTD surrounding the fovea, as seen on the *en face* SS-OCT image (**E1**) and respective outline (**E4**). **(F1-F4)** At the 57-month follow-up visit, the large combined hyperTD continues to grow toward the foveal center. In addition, a fifth hyperTD appears as shown on the *en face* SS-OCT image (**F1**) and respective outline (**F4**). **(G1-G4)** At the 72-month follow-up visit, the fifth hyperTD combines with the merged lesions and form one large hyperTD that has encompassed the foveal center as shown on the *en face* SS-OCT image (**G1**) and respective outline (**G4**).

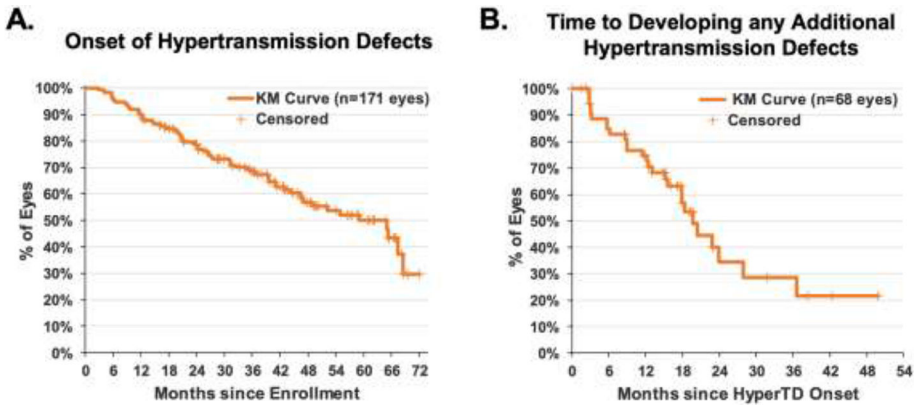

Figure 3:

Kaplan-Meier curves showing the cumulative proportion of iAMD eyes that started with only drusen at baseline and developed at least one persistent choroidal hypertransmission defect (hyperTD) over time **(A)**, and eyes that developed additional hyperTDs after the detection of the first hyperTD **(B)**. Eyes that did not develop any hyperTD were censored at the last follow-up visit. Of the 171 eyes being followed, 68 eyes (39.8%) had developed at least one hyperTD and 27 eyes (15.8%) had developed additional hyperTDs after the first lesion was detected. The median time to hyperTD onset was 59.1 months (95%CI: 46.6 to 68.6). Among the 68 eyes that developed hyperTDs, the median time to developing new hyperTDs was 19.7 months (95%CI: 15.6 to 27.9) with 25% of eyes developing new hyperTDs within a year of the onset.

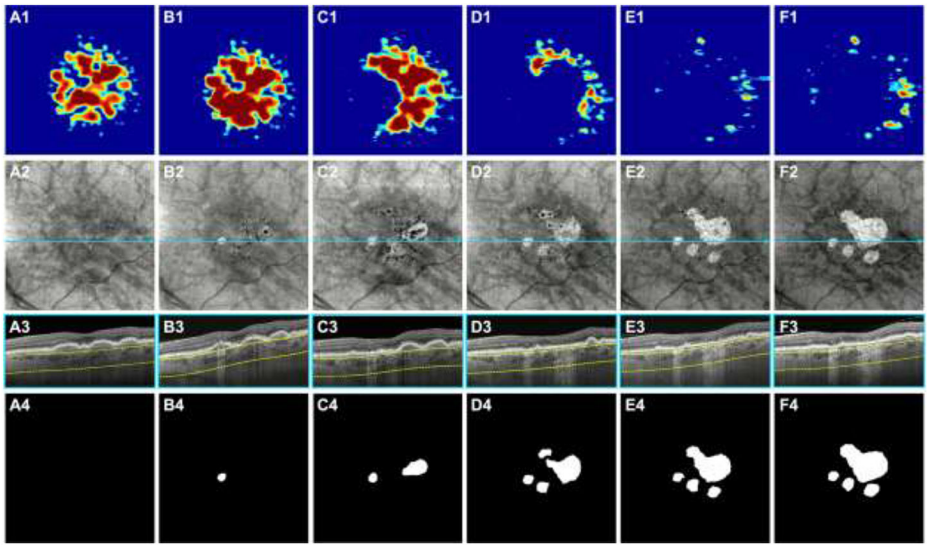

Figure 4:

Swept-source OCT (SS-OCT) imaging of the left eye from a 79-year-old woman beginning with intermediate age-related macular degeneration (iAMD) and progressing to persistent choroidal hypertransmission defects (hyperTDs) over a 60-month period. Column **A** represents the baseline visit, column **B** represents the 18-month follow-up visit, column **C** represents the 24-month follow-up visit, column **D** represents the 28-month follow-up visit, column **E** represents the 48-month follow-up visit, and column **F** represents the 60-month follow-up visit. Row **1** shows the drusen volume maps. Row **2** shows the *en face* SS-OCT structural images that were created using a slab positioned from 64 to 400 μm under Bruch's membrane. Row **3** shows the B-scans corresponding to the color-coded lines in the *en face* SS-OCT images. Row **4** shows the outlines of the hyperTDs that were generated by the algorithm and were manually edited if needed. **(A1-A4)** At the baseline visit, drusen are present as shown by the drusen volume map (**A1**) and respective B-scan (**A3**). There are no hyperTDs present at this visit (**A2** and **A4**). **(B1-B4)** At the 18-month follow-up visit, a hyperTD appears on the *en face* SS-OCT image (**B2**) and is confirmed with the respective B-scan showing hypertransmission below the choroid (**B3**). The respective outline of the hyperTD is shown (**B4**). In addition, hypotransmission defects (hypoTDs) or dark areas on the *en face* image are present which represents hyperpigmentation, and some are shown on the respective B-scan as a thickened RPE layer (**B3**). **(C1-C4)** At the 24-month follow-up visit, a second hyperTD emerges on the *en face* SS-OCT image (**C2**) and is shown on the respective outline (**C4**). In addition, some of the drusen have collapsed at this visit as shown by the drusen volume map (**C1**). **(D1-D4)** At the 28-month follow-up visit, the existing hyperTDs have enlarged with two more hyperTDs appearing as shown on the *en face* SS-OCT image (**D2**) and respective outline (**D4**). In addition, most of the drusen have disappeared at this visit (**D1**). **(E1-E4)** At the 48-month follow-up visit, the hyperTDs have continued to enlarge with two of them merging together. In addition, a fifth hyperTD appears at this visit and is shown on the *en face* SS-OCT image (**E2**) and respective outline (**E4**). **(F1-F4)** At the 60-month follow-up visit, the hyperTDs have continued to enlarge toward the foveal center (**F2** and **F4**).

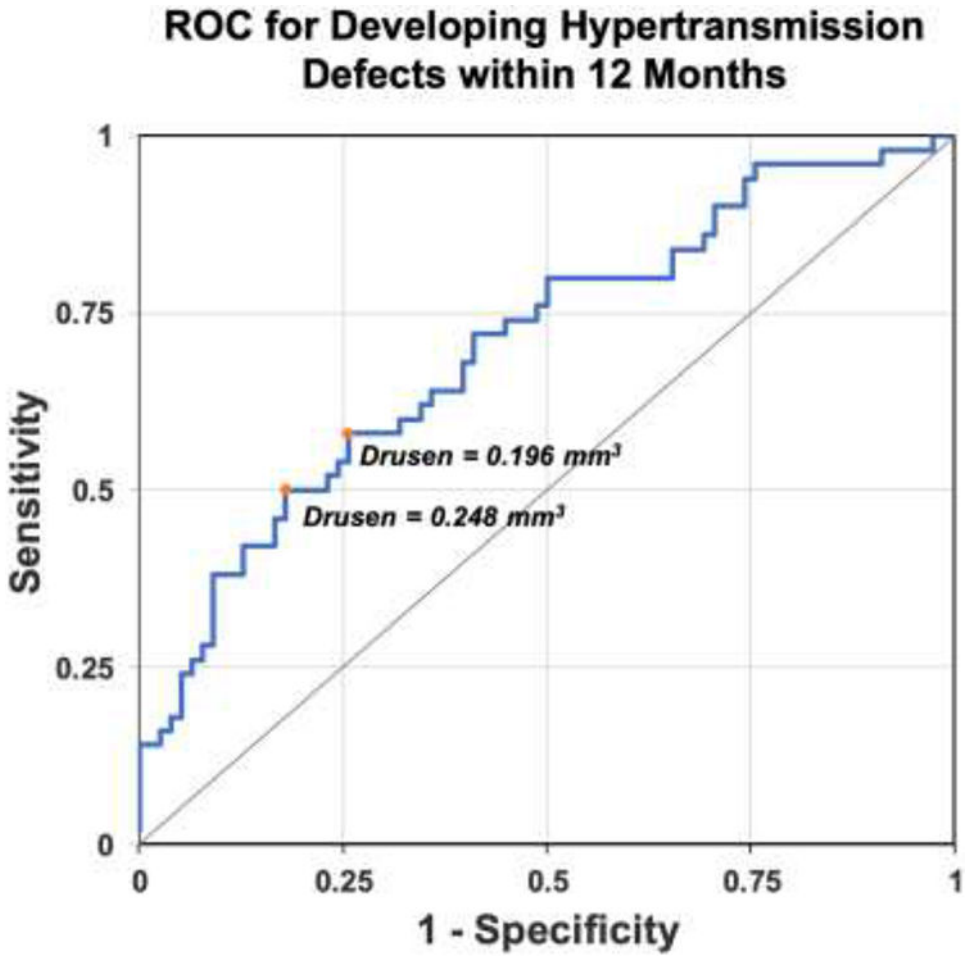

Figure 5:

Receiver operating characteristic (ROC) curve using drusen volume as a risk factor to determine the proportion of cases that would develop persistent choroidal hypertransmission defects (hyperTDs) within 12 months. The gray diagonal line connecting (0,0) to (1,1) is the ROC curve corresponding to random chance (area under the curve [AUC] = 0.5). The blue line represents the ROC curve using drusen volume within the 5 mm circle centered on the fovea as a factor to determine the proportion of cases that would develop hyperTDs in 12 months. The orange dots mark the points on the blue line that are furthest away from the gray diagonal line and identify the optimal drusen volume cutoffs. The chance of developing hyperTDs within 12 months was 58.3% for eyes with a drusen volume ≥ 0.20 mm^3 and 63.2% for eyes with a drusen volume ≥ 0.25 mm^3. The drusen volume within a 5 mm circle centered on the fovea at 9 to 15 months prior to the onset of hyperTDs or the censored timepoint comprised the analysis dataset for the ROC. The drusen volume nearest to 12 months was used if there were multiple assessments within 9 to 15 months.

Table 1:

Number of subjects needed with new onset persistent choroidal hypertransmission defects (hyperTDs) in at least one eye to identify a predicted decrease in growth rate over one year for a given therapy

Power/Alpha	Number of subjects with new onset hyperTDs needed for each treatment group to demonstrate a decrease in the annual growth rate[a]			
	50% decrease in growth rate	40% decrease in growth rate	30% decrease in growth rate	20% decrease in growth rate
80%/0.10	42	65	115	257
80%/0.05	53	83	146	325
90%/0.10	58	90	158	355
90%/0.05	71	110	194	435

[a]Based on 2-sided t-test with an estimated control growth rate (SD) of 0.22 (0.20) mm/year using the square-root transformation strategy for new onset hypertransmission defects (hyperTDs) when comparing the subjects in the highest dose group with the subjects in the placebo-control group at one year.

Table 2:

Baseline number of subjects with intermediate AMD and a minimum drusen volume in at least one eye needed to have the required number of eyes with at least one persistent choroidal hypertransmission defect (hyperTD) by one year of follow-up to determine if a given therapy slows the growth rate of hyperTDs by 50% over one year

Minimum Drusen Volume at Baseline (mm^3)	Number of subjects needed in each treatment group at baseline to achieve the target number of eyes with any hyperTDs by one year[a]			
	80% Power/ Alpha 0.10	80% Power/ Alpha 0.05	90% Power/ Alpha 0.10	90% Power/ Alpha 0.05
0.200	72	91	99	121
0.250	67	84	92	113

[a]Based on an estimated treatment effect that slows the growth rate of hypertransmission defects (hyperTDs) by 50% (Table 1) assuming different statistical powers and alphas to detect the difference between the highest dose group and the placebo group.